Tokyo Climate Center, Japan Meteorological Agency

TCC News

No. 38 Autumn 2014

Contents	Page

El Niño Outlook (October 2014 – April 2015)

The possibility of El Niño condition development during the Northern Hemisphere autumn and winter is comparable to that of continued ENSO-neutral conditions. *(This article was written based on El Nino outlook issued on 10 October 2014.)*

El Niño/La Niña

In September 2014, the NINO.3 SST was near normal with a deviation of +0.4°C. SSTs (Figures 1 and 3 (a)) were remarkably above normal in the western equatorial Pacific, while subsurface temperatures (Figures 2 and 3 (b)) were above normal in most regions from the western to the eastern equatorial Pacific. Atmospheric convective activity was near normal from near the date line to the eastern equatorial Pacific, and easterly winds in the lower troposphere were also near normal in the central equatorial Pacific. These oceanic and atmospheric observations indicate that ENSO-neutral conditions continued in the equatorial Pacific.

Warm subsurface waters in the equatorial Pacific in September tend to support warmer-than-normal SSTs in the eastern part. According to JMA's El Niño prediction model, the NINO.3 SST will be near or above normal during the Northern Hemisphere autumn and winter (Figure 4). In conclusion, the possibility of El Niño condition development during the Northern Hemisphere autumn and winter is comparable to that of continued ENSO-neutral conditions.

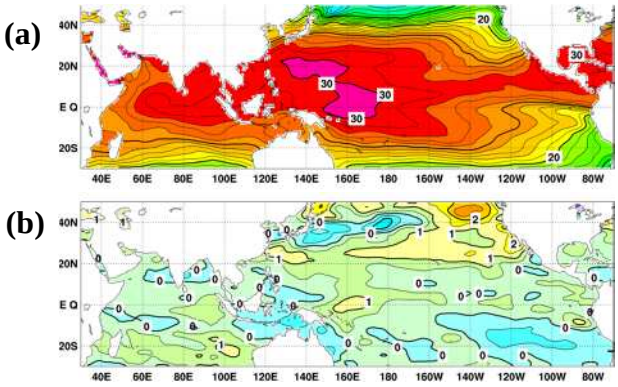

Figure 1 Monthly mean (a) sea surface temperatures (SSTs) and (b) SST anomalies in the Indian and Pacific Ocean areas for September 2014

The contour intervals are 1˚C in (a) and 0.5˚C in (b). The base period for the normal is 1981 – 2010.

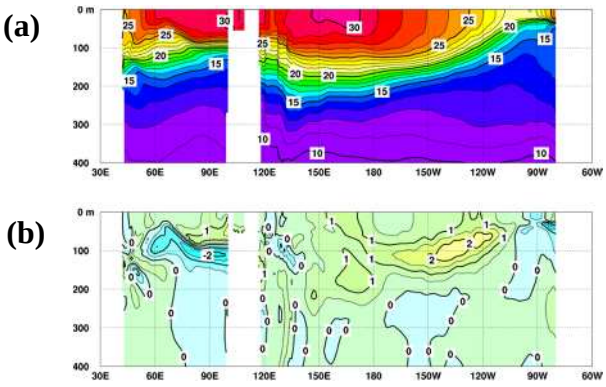

Figure 2 Monthly mean depth-longitude cross sections of (a) temperatures and (b) temperature anomalies in the equatorial Indian and Pacific Ocean areas for September 2014

The contour intervals are 1˚C in (a) and 0.5˚C in (b). The base period for the normal is 1981 – 2010.

Western Pacific and Indian Ocean

The area-averaged SST for the tropical western Pacific (NINO.WEST) region was near normal in September, and is likely to be near or below normal in the Northern Hemisphere autumn and winter.

The area-averaged SST in the tropical Indian Ocean (IOBW) region was near normal in September, and is likely to be near normal in the Northern Hemisphere autumn and winter.

(Ichiro Ishikawa, Climate Prediction Division)

* The SST normal for NINO.3 region (5°S – 5°N, 150°W – 90°W) is defined as the monthly average over a sliding 30-year period (1983-2012 for this year).
* The SST normals for the NINO.WEST region (Eq. – 15°N, 130°E – 150°E) and the IOBW region (20°S – 20°N, 40°E – 100°E) are defined as linear extrapolations with respect to a sliding 30-year period, in order to remove the effects of significant long-term warming trends observed in these regions.

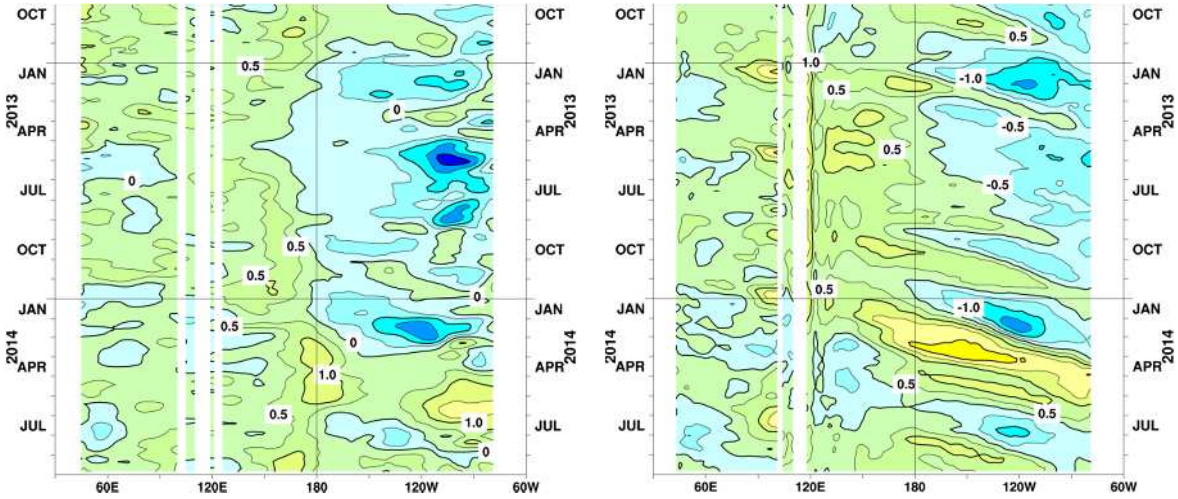

Figure 3 Time-longitude cross sections of (a) SST and (b) ocean heat content (OHC) anomalies along the equator in the Indian and Pacific Ocean areas

OHCs are defined here as vertical averaged temperatures in the top 300 m. The base period for the normal is 1981 – 2010.

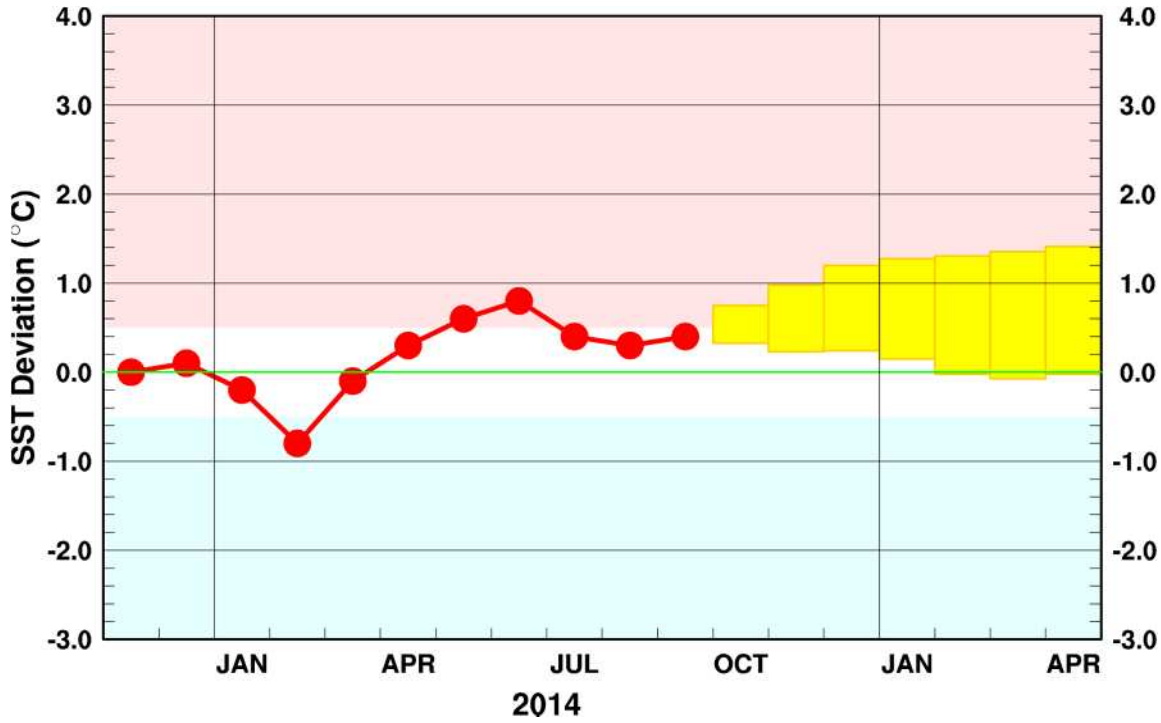

Figure 4 Outlook of NINO.3 SST deviation produced by the El Niño prediction model

This figure shows a time series of monthly NINO.3 SST deviations. The thick line with closed circles shows observed SST deviations, and the boxes show the values produced for the next six months by the El Niño prediction model. Each box denotes the range into which the SST deviation is expected to fall with a probability of 70%.

JMA's Seasonal Numerical Ensemble Prediction for Winter 2014/2015

According to JMA's seasonal ensemble prediction system, sea surface temperature (SST) anomalies in the central and eastern equatorial Pacific Ocean will be significantly above normal this boreal winter, suggesting ongoing El Niño-like conditions. In line with this prediction, active convection over the central Pacific is strongly expected. Conversely, inactive convection is expected over the Maritime Continent and the northern part of the Indian Ocean. The subtropical jet stream over the Eurasian Continent is consequently expected to shift southward.

1. Introduction

This article outlines JMA's dynamical seasonal ensemble prediction for boreal winter 2014/2015 (December 2014 – February 2015, referred to as DJF), which was used as a basis for the Agency's operational warm-season outlook issued on 25 October 2014. The outlook detailed here is based on the seasonal ensemble prediction system of the Coupled Atmosphere-ocean General Circulation Model (CGCM). See the column below for system details.

Section 2 outlines global SST anomaly predictions, and Section 3 describes the associated circulation fields expected over the tropics and sub-tropics. Finally, the circulation fields predicted for the mid- and high- latitudes of the Northern Hemisphere are discussed in Section 4.

2. SST anomalies (Figure 5)

Figure 5 shows predicted SSTs and related anomalies for DJF. Anomalies in the central and eastern equatorial Pacific Ocean appear significantly above normal throughout the period, suggesting ongoing El Niño-like conditions. Conversely, SST anomalies appear slightly below normal around the Philippines, and are also expected to be slightly above normal in the northern part of the Indian Ocean.

3. Prediction for the tropics and sub-tropics (Figure 6)

Figure 6 (a) shows predicted precipitation and related anomalies for DJF. In association with the expected El Niño-like conditions, precipitation amounts over the central equatorial Pacific Ocean are expected to be significantly above normal. Conversely, amounts around the Maritime Continent are expected to be below normal.

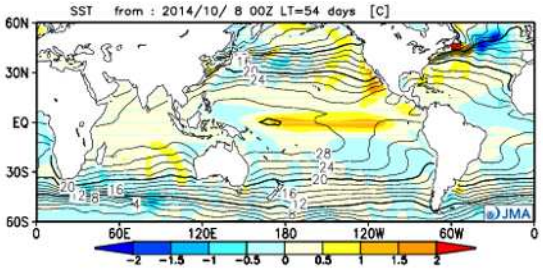

Figure 5 Predicted SSTs (contours) and SST anomalies (shading) for December 2014 – February 2015 (ensemble mean of 51 members)
The contour interval is 2°C.

(a) Precipitation

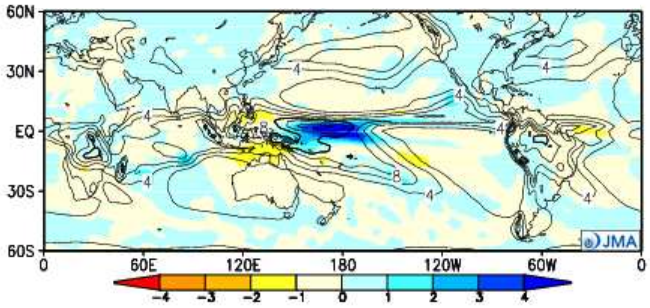

(b) CHI200

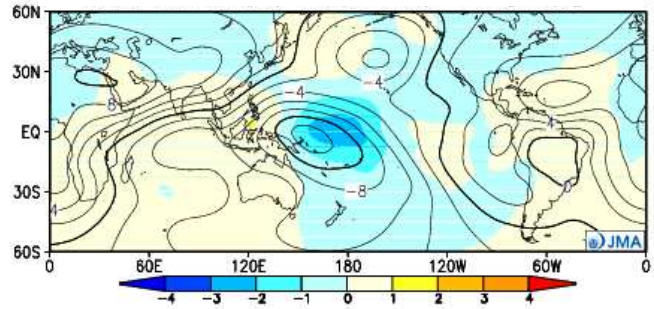

(c) PSI200

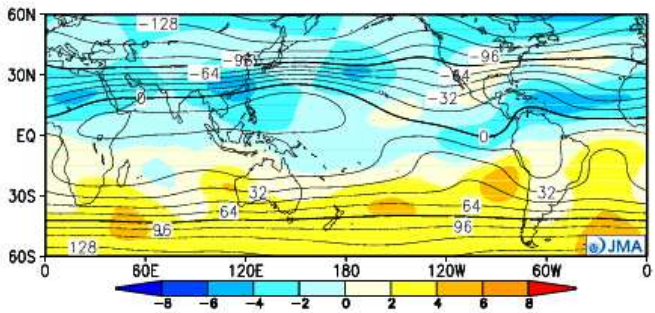

(d) PSI850

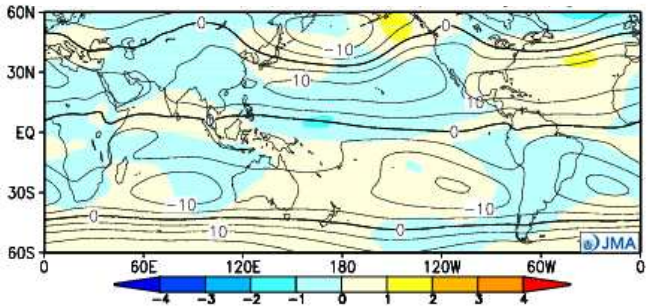

Figure 6 Predicted atmospheric fields from 60°N – 60°S for December 2014 – February 2015 (ensemble mean of 51 members)

(a) Precipitation (contours) and anomaly (shading). The contour interval is 2 mm/day.

(b) Velocity potential at 200 hPa (contours) and anomaly (shading). The contour interval is 2×10^6 m^2/s.

(c) Stream function at 200 hPa (contours) and anomaly (shading). The contour interval is 16×10^6 m^2/s.

(d) Stream function at 850 hPa (contours) and anomaly (shading). The contour interval is 5×10^6 m^2/s.

Velocity potential anomalies in the upper troposphere (200 hPa) (Figure 6 (b)) are expected to be significantly negative (i.e., more divergent) over the central Pacific, reflecting active convection over the central equatorial Pacific Ocean. Conversely, positive (i.e., more convergent) anomalies are expected around the Maritime Continent and the northern part of the Indian Ocean, reflecting inactive convection in these regions.

Stream function anomalies at 200 hPa (Figure 6 (c)) are expected to be zonally negative (i.e., cyclonic) over the Eurasian Continent, indicating a tendency of southward shift for the subtropical jet stream.

Stream function anomalies at 850 hPa (Figure 6 (d)) are expected to be negative (i.e., cyclonic) over the central equatorial Pacific, reflecting active convection in the region.

4. Prediction for the mid- and high latitudes of the Northern Hemisphere (Figure 7)

Geo-potential height anomalies at 500 hPa (Figure 7 (a)) are expected to be positive over most of the Northern Hemisphere's mid-latitude region, reflecting positive Arctic Oscillation (AO). However, this should be interpreted with caution because the reliability of positive AO prediction is limited.

Sea level pressure anomalies (Figure 7 (b)) are expected to be positive in the North Pacific and negative around Siberia. As a result, the Aleutian Low and the Siberian High are expected to be weaker than normal, suggesting a weaker-than-normal Asian winter monsoon. However, this should also be interpreted with caution because these phenomena are affected by unpredictable mid- and high- latitude wave activity.

(Takashi Yamada, Climate Prediction Division)

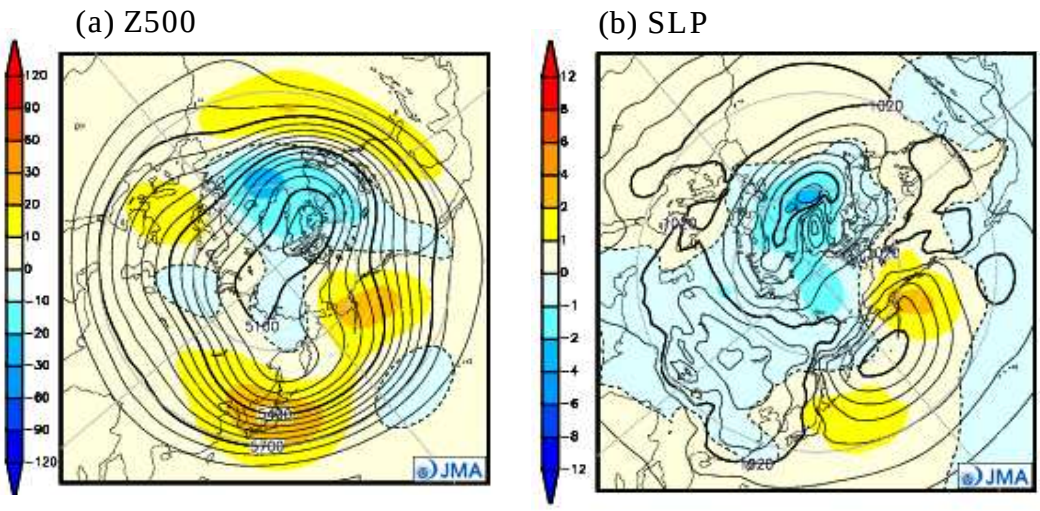

Figure 7 Predicted atmospheric fields from 20°N – 90°N for December 2014 – February 2015 (ensemble mean of 51 members)
(a) Geopotential height at 500 hPa (contours) and anomaly (shading). The contour interval is 60 m.
(b) Sea level pressure (contours) and anomaly (shading). The contour interval is 4 hPa.

JMA's Seasonal Ensemble Prediction System

JMA operates a seasonal Ensemble Prediction System (EPS) using the Coupled atmosphere-ocean General Circulation Model (CGCM) to make seasonal predictions beyond a one-month time range. The EPS produces perturbed initial conditions by means of a combination of the initial perturbation method and the lagged average forecasting (LAF) method. The prediction is made using 51 members from the latest six initial dates (nine members are run every five days). Details of the prediction system and verification maps based on 30-year hindcast experiments (1979 – 2008) are available at http://ds.data.jma.go.jp/tcc/tcc/products/model/.

Cold Season Outlook for Winter 2014/2015 in Japan

In winter 2014/2015, mean temperatures are expected to be near or above normal, both with 40% probability, in western Japan and Okinawa/Amami. Cold-season precipitation amounts are expected to be near or above normal, both with 40% probability, on the Pacific side of western Japan and in Okinawa/Amami.

1. Outlook summary (Figure 8)

JMA issued its outlook for the coming winter (December 2014 – February 2015) over Japan in September and updated it on 24 October based on the output of its seasonal Ensemble Prediction System (EPS). This article summarizes the update.

According to the outlook, mean temperatures in winter 2014/2015 will be near or above normal, both with 40% probability, in western Japan and Okinawa/Amami, and near normal in eastern and northern Japan. Cold-season precipitation amounts are expected to be near or above normal, both with 40% probability, on the Pacific side of western Japan and in Okinawa/Amami, and to be near normal over the remaining region. Snowfall amounts for the Sea of Japan side are expected to be near or below normal, both with 40% probability, in western Japan, and near normal in northern and eastern Japan.

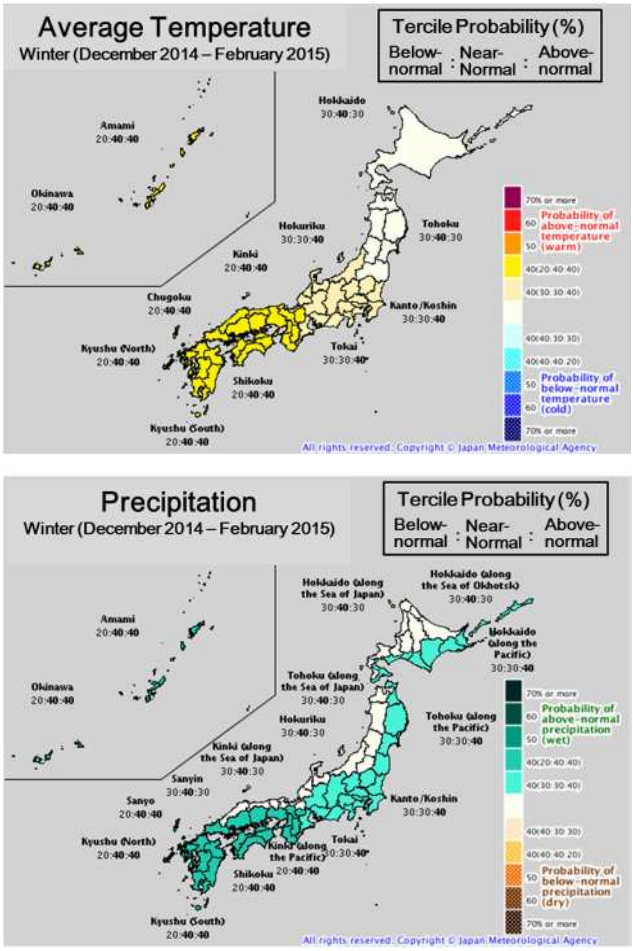

Figure 8 Outlook for winter 2014/2015 temperature (above) and precipitation (below) probability in Japan.

2. Outlook background

The schematic diagram in Figure 9 shows expected large-scale characteristics of the ocean and atmosphere for this winter. The background to the outlook is summarized below.

- Sea surface temperatures are expected to be above normal from west of the date line to the eastern part of the equatorial Pacific. According to the El Niño Outlook, the possibility of El Niño condition development during the coming winter season is comparable to that of continued ENSO-neutral conditions.
- Convective activity in the tropics is expected to be stronger than normal around the date line in the tropical Pacific and weaker than normal from the Indian Ocean to the Maritime continent.
- The subtropical jet stream is expected to shift southward over the Eurasian continent in association with inactive convection from the Indian Ocean to the Maritime continent. Accordingly, northeastward anomalies of the upper flow are expected over west of Japan, which is likely to be influenced more than normal by low pressure.
- The Aleutian low is expected to shift southeastward of its climatological location.
- The model predicts a positive AO pattern and a tendency of weakness in the Siberian High. However, forecasters interpret this expectation in consideration of prediction skill based on hindcasting.
- In consideration of all relevant factors, the northwesterly monsoon is expected to be near normal from northern to eastern Japan and weaker than normal over western Japan and Okinawa/Amami.

(Masayuki Hirai, Climate Prediction Division)

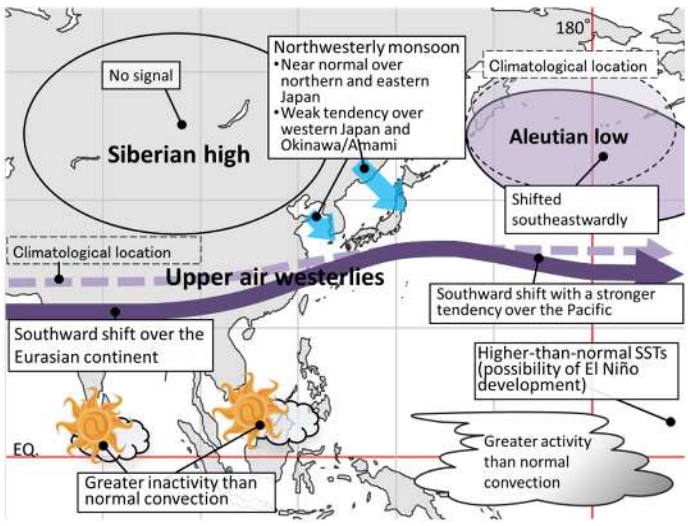

Figure 9 Schematic diagram showing expected large-scale characteristics of the ocean and atmosphere in winter 2014/15

Summary of the 2014 Asian Summer Monsoon

1. Precipitation and temperature

Four-month total precipitation amounts based on CLIMAT reports during the monsoon season (June – September) were more than 120% of the normal in Hokkaido region of Japan, from western Japan to southern China and from western China to northern Pakistan. Conversely, the corresponding figures were less than 60% of the normal around the Korean Peninsula, in central and northwestern Mongolia, in southern parts of Central Asia and in southern Pakistan (Figure 10). The amounts were mostly consistent with the distribution of four-month mean OLR anomalies (Figure 12).

Extremely heavy precipitation was seen from western Japan to southern China and in southwestern India in August. In contrast, extremely light precipitation was seen in Mongolia in July (figures not shown).

Four-month mean temperatures for the same period were more than 1°C above normal in Japan's Hokkaido region, southeastern Mongolia, southeastern China, central India and western Pakistan, and were more than 1°C below normal around eastern China and northern Mongolia (Figure 11).

Heavy rain reportedly caused fatal floods and landslides in western India in July, in Nepal and adjacent northern India in August, and around the border of India and Pakistan in September. Monsoon season fatalities were reported as exceeding 1,000 in India, 250 in Nepal and 360 in Pakistan.

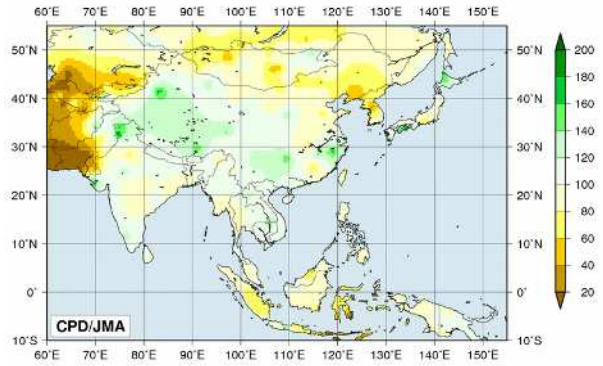

Figure 10 Four-month precipitation ratios (%) from June to September 2014

The base period for normal is 1981 – 2010. There were not data in Afghanistan.

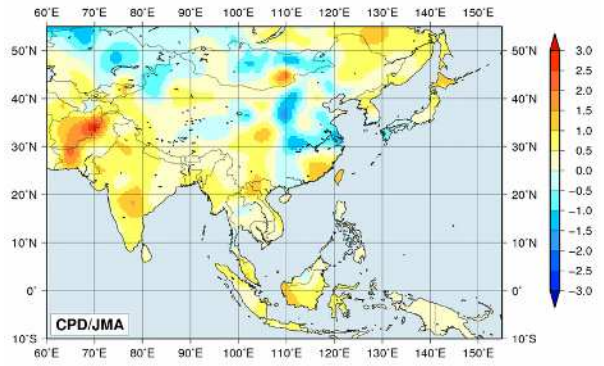

Figure 11 Four-month mean temperature anomalies (°C) from June to September 2014

The base period for normal is 1981 – 2010. There were not data in Afghanistan.

2. Tropical cyclones

During the monsoon season, 13 tropical cyclones (TCs) of tropical storm (TS) intensity or higher formed over the western North Pacific (Table 1). This was lower than the 1981 – 2010 average of 16.0. A total of 5 among these 13 passed around the South China Sea and approached or hit Viet Nam or China, 3 passed over the Philippines and 2 hit the main islands of Japan.

Fatalities caused by Typhoon Rammasun exceeded 100 in the Philippines, 20 in Viet Nam and 50 in China.

Note: Disaster information is based on reports by governmental organizations (China, India, Nepal, Pakistan and the Philippines) and the European Commission.

Table 1 Tropical cyclones forming over the western North Pacific from June to September 2014

Number ID	Name	Date (UTC)	Category[1)]	Maximum wind[2)] (knots)
T1406	Mitag	6/11 – 6/11	TS	40
T1407	Hagibis	6/14 – 6/17	TS	40
T1408	Neoguri	7/3 – 7/10	TY	100
T1409	Rammasun	7/12 – 7/19	TY	90
T1410	Matmo	7/17 – 7/25	TY	70
T1411	Halong	7/29 – 8/10	TY	105
T1412	Nakri	7/29 – 8/3	STS	55
T1413	Genevieve	8/7 – 8/12	TY	110
T1414	Fengshen	9/6 – 9/10	STS	60
T1415	Kalmaegi	9/12 – 9/17	TY	75
T1416	Fung-wong	9/17 – 9/23	TS	45
T1417	Kammuri	9/24 – 9/30	STS	50
T1418	Phanfone	9/29 – 10/6	TY	95

Note: Based on information from the RSMC Tokyo-Typhoon Center.
1) Intensity classification for tropical cyclones
TS: Tropical storm, STS: Severe tropical storm, TY: Typhoon
2) Estimated maximum 10-minute mean wind

3. Monsoon activity and atmospheric circulation

Convective activity (inferred from OLR) averaged for June – September 2014 was enhanced over the southern part of the South China Sea and around the southwestern part of Japan, and was suppressed over western to central parts of the equatorial Indian Ocean, India, the Bay of Bengal and around Taiwan (Figure 12). According to the OLR indices (Table 2), the overall activity of the Asian summer monsoon (represented by the SAMOI (A) index) was below normal except in July. Convective activity in the vicinity of the Philippines was characterized by distinct intra-seasonal variability with an enhanced phase in July in contrast to a suppressed phase in August, as implied by the negative-to-positive shift in SAMOI (W).

In the upper troposphere, the Tibetan High was generally weaker than normal (Figure 13 (a)), which was consistent with the subtropical jet stream flowing southward of its normal position. In the lower troposphere the monsoon trough was prominent east of the Philippines. Zonal wind shear between the upper and lower atmosphere over the North Indian Ocean and southern Asia (Figure 14) was enhanced in mid-July and reduced in mid-August. The northwestward extension of the Pacific High was weaker than normal, which was a contributing factor to cool and wet summer conditions around western Japan (Figure 13 (b)).

(Sections 1 and 2: Ayako Takeuchi, 3: Yoshinori Oikawa, Tokyo Climate Center)

References

Webster, P. J. and S. Yang, 1992: Monsoon and ENSO: Selectively interactive systems. *Quart. J. Roy. Meteor. Soc.*, **118**, 877 – 926.

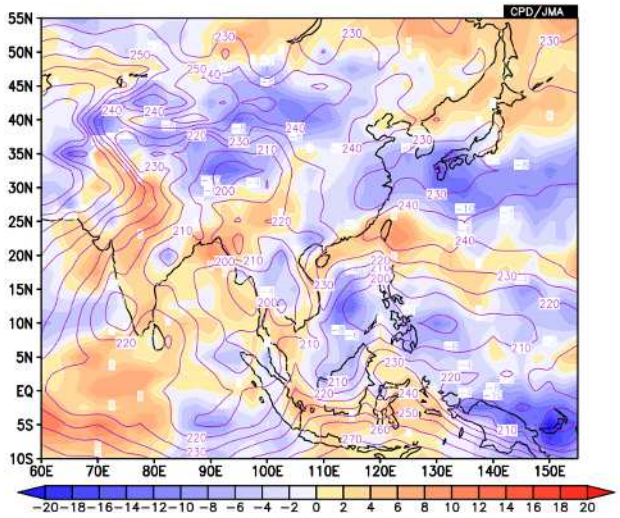

Figure 12 Four-month mean OLR and its anomaly for June–September 2014

The contours indicate OLR at intervals of 10 W/m^2, and the color shading denotes OLR anomalies from the normal (i.e., the 1981–2010 average). Negative (cold color) and positive (warm color) OLR anomalies show enhanced and suppressed convection compared to the normal, respectively. Original data are provided by NOAA.

Table 2 Summer Asian Monsoon OLR Index (SAMOI) values observed from May to October 2014

Asian summer monsoon OLR indices (SAMOI) are derived from OLR anomalies from May to October. SAMOI (A), (N) and (W) indicate the overall activity of the Asian summer monsoon, its northward shift and its westward shift, respectively. SAMOI definitions are as follows: SAMOI (A) = (-1) × (W + E); SAMOI (N) = S – N; SAMOI (W) = E – W. W, E, N and S indicate area-averaged OLR anomalies for the respective regions shown in the figure on the right normalized by their standard deviations.

	Summer Asian Monsoon OLR Index (SAMOI)		
	SAMOI (A): Activity	SAMOI (N): Northward-shift	SAMOI (W): Westward-shift
May 2014	-0.5	-0.4	1.9
Jun. 2014	-0.4	-0.4	-0.6
Jul. 2014	1.5	0.3	-1.3
Aug. 2014	-0.6	-0.5	1.0
Sep. 2014	-0.1	-0.6	-0.9
Oct. 2014	-0.4	-0.2	-0.4

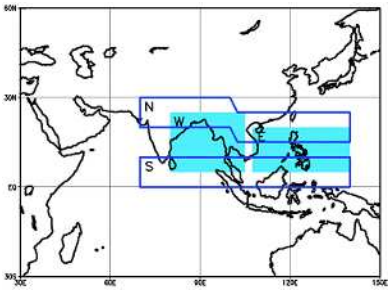

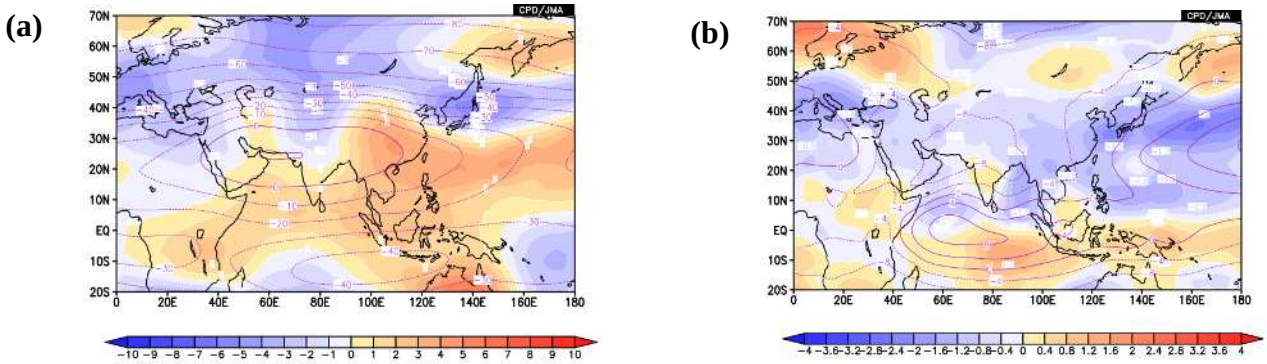

Figure 13 Four-month mean stream function and its anomaly for June – September 2014

(a) The contours indicate the 200-hPa stream function at intervals of 10 × 10^6 m^2/s, and the color shading indicates 200-hPa stream function anomalies from the normal. (b) The contours indicate the 850-hPa stream function at intervals of 4 × 10^6 m^2/s, and the color shading indicates 850-hPa stream function anomalies from the normal. The base period for the normal is 1981 – 2010. Warm (cold) shading denotes anticyclonic (cyclonic) circulation anomalies in the Northern Hemisphere, and vice-versa in the Southern Hemisphere.

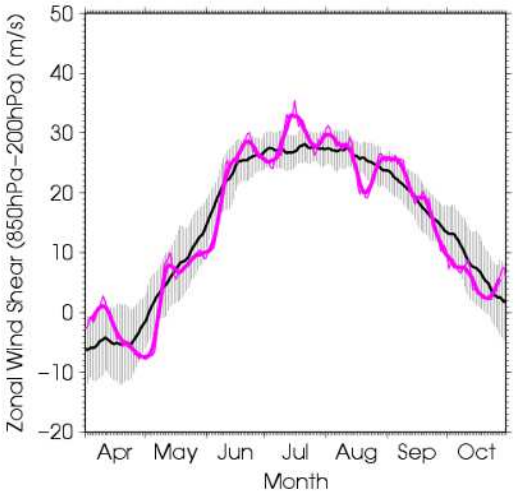

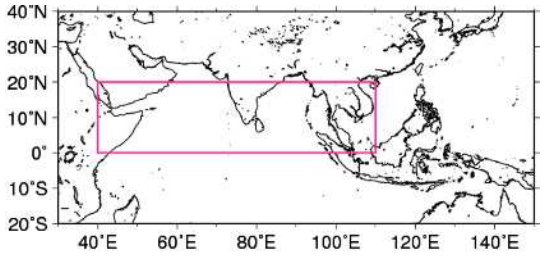

Figure 14 Time-series representation of the zonal wind shear index between 200-hPa and 850-hPa averaged over the North Indian Ocean and southern Asia (the region enclosed by the pink rectangle in the right figure: equator – 20°N, 40°E – 110°E)

The zonal wind shear index is calculated after Webster and Yang (1992). The thick and thin pink lines indicate seven-day running mean and daily mean values, respectively. The black line denotes the normal (i.e., the 1981 – 2010 average), and the gray shading shows the range of the standard deviation calculated for the time period of the normal.

Status of the Antarctic Ozone Hole in 2014

The size of the Antarctic ozone hole in 2014 was equivalent to its average over the last 10 years.

Over the last 30 years, the Antarctic ozone hole has appeared every year in Austral spring with a peak in September or early October. Its scale is generally represented by the area in which the total ozone column is equal to or less than 220 m atm-cm.

According to JMA's analysis based on data from National Aeronautics and Space Administration (NASA) satellites, the Antarctic ozone hole in 2014 appeared in mid-August and expanded rapidly from late August to mid-September before temporarily contracting then expanding again in late September, reaching its maximum size for the year on 1 October. At this time it covered 23.4 million square kilometers (see the upper left panel in Figure 15), which is 1.7 times as large as the Antarctic Continent. The scale of the hole in 2014 was equivalent to the average over the last ten years, and its maximum size was almost the same as that of 2013 (upper-right panel). The bottom panels in Figure 15 indicate the development of this year's ozone hole.

The ozone layer acts as a shield against ultraviolet radiation, which can cause skin cancer. The ozone hole first appeared in the early 1980s and reached its maximum size of 29.6 million square kilometers in 2000. It is expected to continue to appear over the Antarctic at least until the middle of this century, and has caused significant changes in the Southern Hemisphere's summer surface climate according to WMO/UNEP Scientific Assessment of Ozone Depletion: 2014 Assessment for Decision-Makers. Close observation of the ozone layer both over the Antarctic region and globally remains important.

(Atsuya Kinoshita, Ozone Layer Monitoring Center)

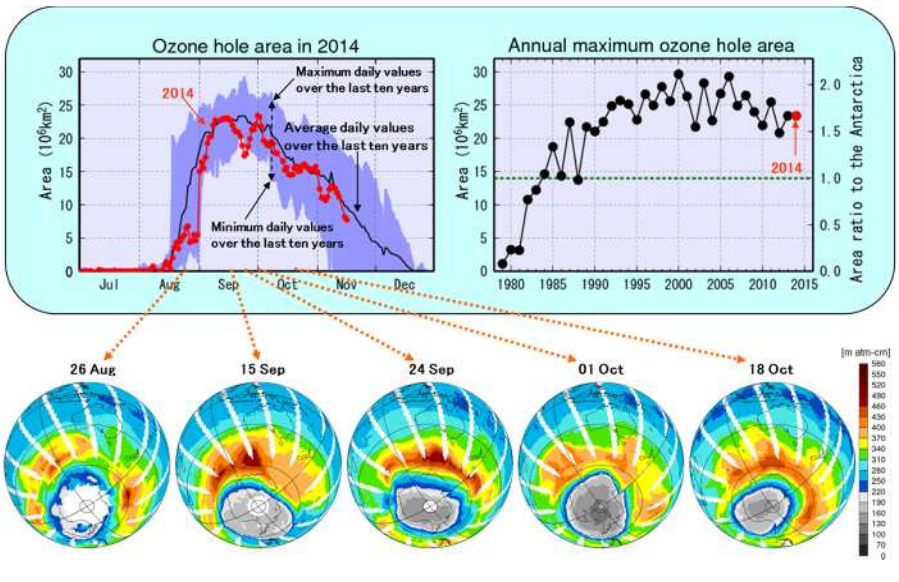

Figure 15
Antarctic ozone hole characteristics

Upper left: Time-series representation of the daily ozone-hole area for 2014 (red line) and the 2004–2013 average (black line). The blue shading area represents the range of daily minima and daily maxima over the past 10 years. Upper right: Interannual variability in the annual maximum ozone-hole area. Bottom: Snapshots of total column ozone distribution on selected days in 2014; the ozone hole is shown in gray. These panels are based on data from NASA satellite sensors of the total ozone mapping spectrometer (TOMS) and ozone monitoring instrument (OMI).

New Forecast Products in Support of Early Warnings for Extreme Weather Events

In August 2014, JMA started providing new forecast products via the TCC website to support early warnings for extreme weather events. The products include maps of the Extreme Forecast Index (EFI), extreme weather warnings based on the EFI and probabilistic forecasts for extreme conditions together with the EPSgram covering the period up to two weeks ahead.

Introduction

Early warnings for extreme events on a sub-seasonal time scale are of great benefit in socio-economic activities such as mitigating the effects of floods and heatwaves and ensuring appropriate food and water supplies. TCC developed a set of extreme weather warning products based on JMA's operational one-month ensemble prediction system (EPS) to support the provision of early warnings for extreme events. These products are intended to act as complementary information on weather conditions for decision-makers, and can be used in addition to historical and real-time information from climate monitoring. The new products available on the TCC website are outlined below.

New products

(1) EFI

The Extreme Forecast Index (EFI) was originally developed at ECMWF (Lalaurette, 2002; 2003) to quantitatively indicate how and where EPS forecasts differ from the climatological probability. It expresses the difference between the probability distribution of a real-time forecast and the climatological probability distribution (Lalaurette, 2003) as a simple value ranging from -1 (all forecast members below the 0th percentile of the climatology) to +1 (all forecast members above the 100th percentile). Thanks to its relatively simple and intuitive nature, it is widely used by national weather services. JMA adopted a revised version (Zsótér 2006) of the index for its products. Figure 1 shows a sample EFI map. As the EFI is a signed index, the probabilities of both high and low outliers can be summarized in one simple figure. For more scientific and technical details, see Harada and Takaya (2012). Verification of EFI products is also described in Matsueda and Takaya (2013).

(2) Probabilistic forecast for extreme conditions

Maps of predicted probabilities above the 90th percentile and below the 10th percentile of the model climatology are also displayed along with EFI maps (Figure 16), which can be used to determine the locations and timing of extreme weather conditions.

(3) Extreme weather warning map

A warning map based on probability above/below outliers (i.e., 90th and 10th percentiles) was proposed and applied to THORPEX Interactive Grand Global Ensemble (TIGGE; Bougeault et al. 2010) data by Nakazawa and Matsueda (2010). JMA developed a similar EFI-based warning map showing an integrated view of extreme weather areas where the absolute EFI exceeds thresholds of 0.5 and 0.8 for individual weather parameters (Figure 17).

(4) EPSgram

Time-series representations of EFI and EPSgrams are also provided on the website for selected major cities. EPSgrams show expected ranges from EPS forecasts with boxes representing percentiles along with climatological ranges assessed from hindcasts (Figure 18). This allows users to view the predicted time evolution of extreme events.

(Satoko Matsueda, Masashi Harada[1] and Yuhei Takaya, Climate Prediction Division, [1]currently Marine Division)

The products highlighted here are intended to support NMHSs in Asia and other regions, and are available exclusively to pre-registered users. To inquire about access to these products, contact TCC at tcc@met.kishou.go.jp.

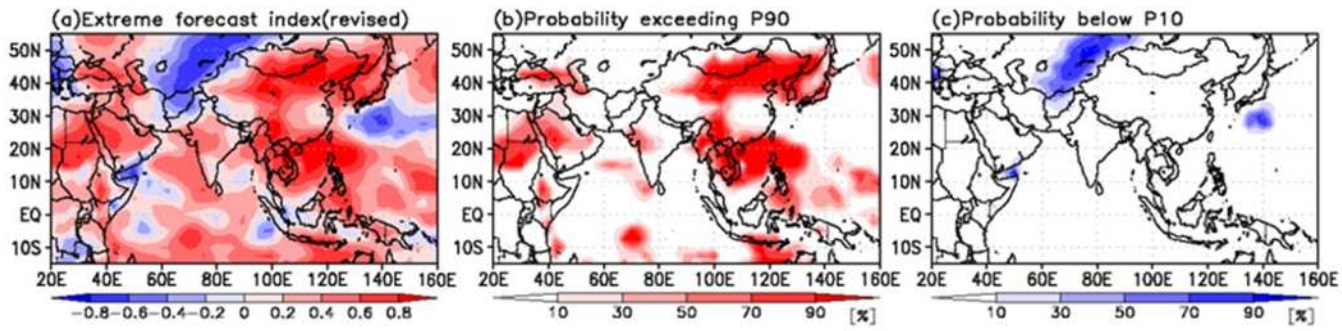

Figure 16 (a) EFI and probabilities (b) above the 90th percentile and (c) below 10th percentile for surface temperature from 29 May to 4 June 2014 as determined from JMA one-month prediction starting on 28 May 2014.
The red (blue) regions indicate a high probability of extremely high (low) temperatures.

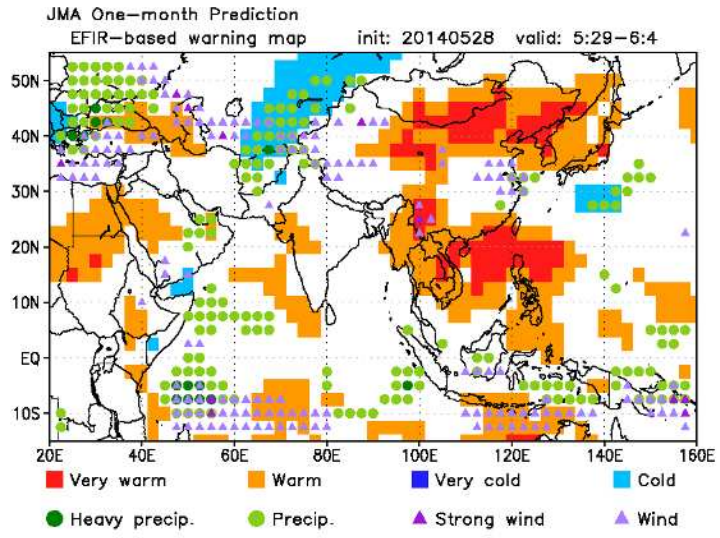

Figure 17 Extreme weather warning map.
Occurrence probabilities for various extreme events are plotted on this map based on the following EFI thresholds:
Very warm, Very cold, Heavy rain and Strong wind: |EFI| ≥ 0.8
Warm, Cold, Precip. and Wind: |EFI| ≥ 0.5
The period and initial date of the forecast are the same as those for Figure 16.

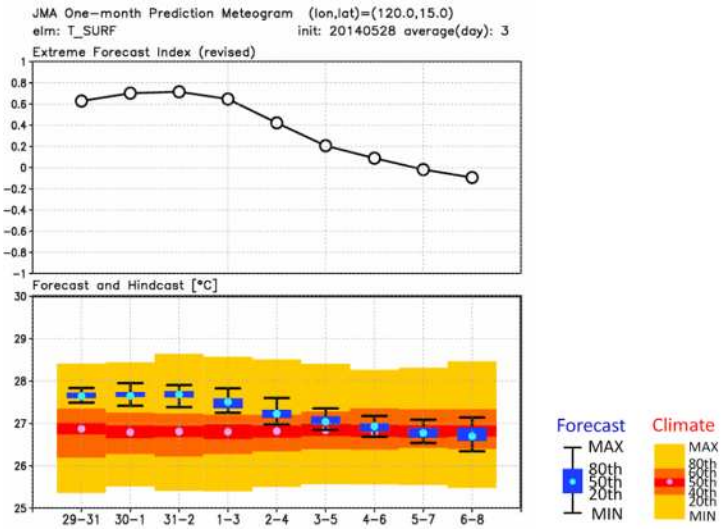

Figure 18 EFI time-series representation and EPSgram for the 3-day averaged temperature at Manila in the Philippines (120°E, 15°N) for the case shown in Figure 16.
(Top) Time-series representation of EFI values. (Bottom) Time-series representation of the EPS forecast (cold color) and the model climate (warm color). EPS forecast distribution is represented by box-whisker plots with the median (light-blue circles), the 20^{th}/80^{th} percentiles (blue boxes) and the minimum and maximum values (whiskers). Model climate distribution is represented by box plots with the median (pink circles), the 40^{th}/60^{th} percentiles (red boxes), the 20^{th}/80^{th} percentiles (orange boxes) and the minimum and maximum values (yellow boxes).

References

Bougeault, P. and co-authors, 2010: The THORPEX Interactive Grand Global Ensemble. *Bull. Amer. Meteor. Soc.*, **91,** 1059–1072.

Harada, M. and Y. Takaya, 2012: Development of Extreme Weather Warning Products with JMA One-month Ensemble Prediction System, CAS/JSC WGNE Research Activities in Atmospheric and Oceanic Modelling, WGNE Blue Book 2012.

Lalaurette, F., 2002: Early detection of abnormal weather conditions using a probabilistic extreme forecast index. ECMWF Tech. Memorandum, 373.

Lalaurette, F., 2003: Early detection of abnormal weather conditions using a probabilistic extreme forecast index. Quart. J. Roy. Meteor. Soc., **129,** 3037 – 3057.

Matsueda, S. and Y. Takaya, 2013: Verification of the Extreme Forecast Index in JMA's Operational One-month Ensemble Prediction System, CAS/JSC WGNE Research Activities in Atmospheric and Oceanic Modelling, WGNE Blue Book 2013.

Nakazawa, T. and M. Matsueda, 2010: Genesis potential estimation of high-impact weather by TIGGE ensemble data. The 29th Conference on Hurricanes and Tropical Meteorology, 15D.1.

Zsótér, E., 2006: Recent developments in extreme weather forecasting. ECMWF Newsletter, **107,** 8 – 17.

Unseasonable weather conditions in Japan in August 2014

– Summary of analysis by the TCC Advisory Panel on Extreme Climatic Events –

In an extraordinary session held at the Japan Meteorological Agency on 3 September 2014, the TCC Advisory Panel on Extreme Climatic Events[1] issued a statement on primary factors causing the cloudy and rainy conditions observed in Japan in August 2014.

- In August 2014, western Japan experienced record-high precipitation and record-low sunshine durations. From 30 July to 26 August, heavy rainfall events were observed throughout the country.
- These weather conditions were caused by continuous southerly warm moist air flow in association with two typhoons moving northward near or over western Japan from late July to early August and with the southward shift and significant meandering of the jet stream around Japan from mid- to late August. This meandering is considered partially attributable to suppressed Asian monsoon activity in association with above-normal sea surface temperatures in the eastern Pacific and the eastern Indian Ocean as well as tropical intra-seasonal oscillation[2].

1. Climatic characteristics (Figures 19 and 20, Table 3)

After 30 July 2014, cloudy and rainy conditions were prominent nationwide except in Okinawa/Amami and the Kanto region.

The monthly precipitation ratio to the normal averaged over the Pacific side of western Japan for August 2014 was 301%, which was the highest since 1946 when collection of the area-averaged statistical data referenced here began. Monthly precipitation ratios were also significantly above normal in northern Japan and on the Sea of Japan side of eastern and western Japan. Heavy rain was brought by two typhoons, fronts and moist air flow, resulting in record-high precipitation at observation stations from Hokkaido in the north to Kyushu in the south.

The monthly sunshine duration ratio to the normal averaged over the Pacific side of western Japan was 54%, which was the lowest since 1946. The ratio averaged over the Sea of Japan side of western Japan was 42%, which was the second lowest after 1980, and the figure was also significantly below normal over eastern Japan.

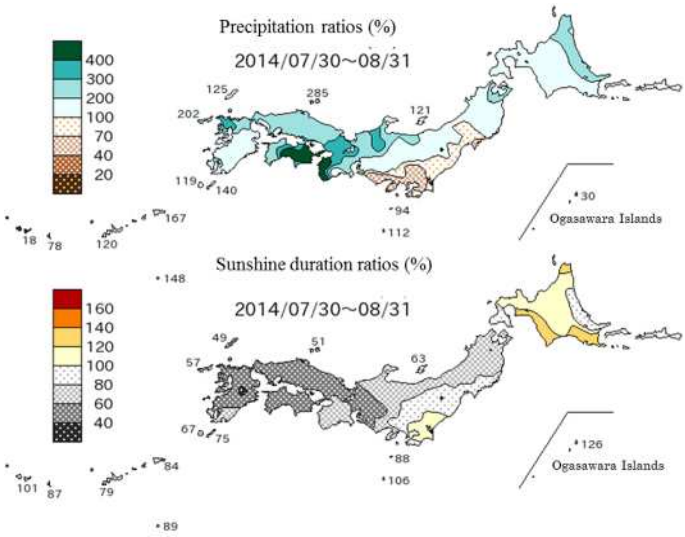

Figure 19 Precipitation ratios and sunshine duration ratios for the period from 30 July to 31 August 2014
The base period for the normal is 1981 – 2010.

Table 3 Regional averages and related rankings of monthly precipitation ratios and monthly sunshine duration ratios for August 2014

August		Precipitation ratio (%)				Sunshine duration ratio (%)			
		2014		Record high (year)		2014		Record low (year)	
Northern Japan	Sea of Japan side	171	[3]	264	(1981)	94		61	(1998)
	Pacific side	156		222	(1998)	94		58	(1998)
Eastern Japan	Sea of Japan side	234	[3]	279	(1976)	58		49	(1993)
	Pacific side	121		209	(1982)	75		54	(1980)
Western Japan	Sea of Japan side	242	[3]	301	(1980)	42	[2]	41	(1980)
	Pacific side	301	[1]	231	(2004)	54	[1]	57	(1980)
Okinawa and Amami		76		252	(2012)	93		73	(1960)

*The numbers in square brackets indicate the ranking for August 2014 since 1946. Rankings of precipitation ratios and sunshine duration ratios are shown in descending and ascending order, respectively.

[1] The Advisory Panel, consisting of prominent experts on climate science from universities and research institutes, was established in June 2007 by JMA to investigate extreme climate events based on up-to-date information and findings. See TCC News No. 9 and No. 28.
[2] In the tropics, enhanced and suppressed areas of large-scale cumulus convection appear alternately in cycles of 30 to 60 days.

2. Characteristic atmospheric circulation causing Japan's unseasonable weather conditions (Figure 21)

(1) General characteristics from late July to August 2014

From late July to August 2014, the Pacific High was enhanced to the southeast of mainland Japan and its westward expansion was weaker than normal, which brought continuous southerly warm moist air flow to the country.

From late July to early August 2014, Typhoon Nakri and Typhoon Halong approached Japan in quick succession. After early August, fronts that tended to linger around the nation's mainland brought above-normal precipitation amounts and below-normal sunshine durations over a wide area of western Japan and other parts of the country, and heavy rainfall events were observed nationwide.

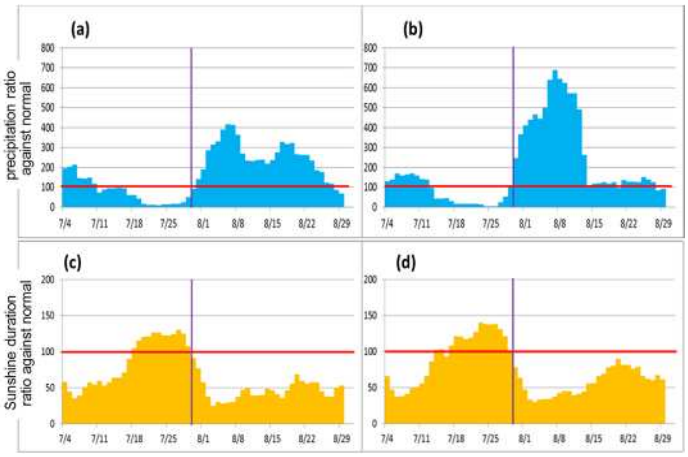

Figure 20 (a) Seven-day running mean precipitation ratios for the Sea of Japan side of western Japan. (b) As per (a), but for the Pacific side of western Japan. (c) As per (a), but for sunshine duration ratios. (d) As per (b), but for sunshine duration ratios.
The red horizontal lines indicate the ratio of 100% to the normal. The purple lines indicate 30 July. The base period for the normal is 1981 – 2010.

(2) Late July to early August 2014

The subtropical jet stream was shifted northward of its normal position around Japan. As a result, Typhoon Nakri did not turn eastward after approaching Japan due to the jet stream's diminished effect. The lasting effects of the typhoon were felt in western and other parts of Japan even after its transformation into an extratropical cyclone.

The Pacific High was enhanced to the southeast of mainland of Japan, which facilitated warm moist air flow over the country along the periphery of the Pacific High. Heightened convective activity around the Philippines is thought to have contributed to the enhanced Pacific High.

(3) Mid- to late August 2014

Typhoon Halong moved slowly northward in the area to the south of western Japan and made landfall over Shikoku on 10 August. After passing over western Japan, it continued northward over the Sea of Japan. In early August, the subtropical jet stream began to shift southward of its normal position around Japan before meandering significantly (i.e., southward meandering to the west of Japan and northward meandering to the east of Japan) toward the middle of the month. In association, fronts tended to linger near the nation's mainland. While the Pacific High was enhanced to the southeast of Japan, its westward expansion was weak. Suppressed cumulus convection over the Asian monsoon region (Southeast Asia and South Asia) in association with the tropical intra-seasonal oscillation is considered to have contributed to the southward shift and meandering of the jet stream.

While convective activity around the Philippines was enhanced during early August, it subsequently became suppressed and continued in this condition. A contributory factor to this situation is considered to be the influence of downward air flow over the western part of the Pacific including the Philippines in association with upward air flow caused by enhanced convective activity in association with above-normal sea surface temperatures in the eastern Pacific and the eastern Indian Ocean. The influence of tropical intra-seasonal oscillations is seen as another contributory factor. In association with positive anomalies of lower tropospheric pressure related to suppressed convective activity around the Philippines, southwesterly warm moist air flow in the lower troposphere from the South China Sea to the East China Sea was predominant, while westerly flow from the South China Sea to the Pacific east of the Philippines is seen in normal years. This southwesterly flow is considered to have contributed to the enhancement of warm moist air inflow over Japan.

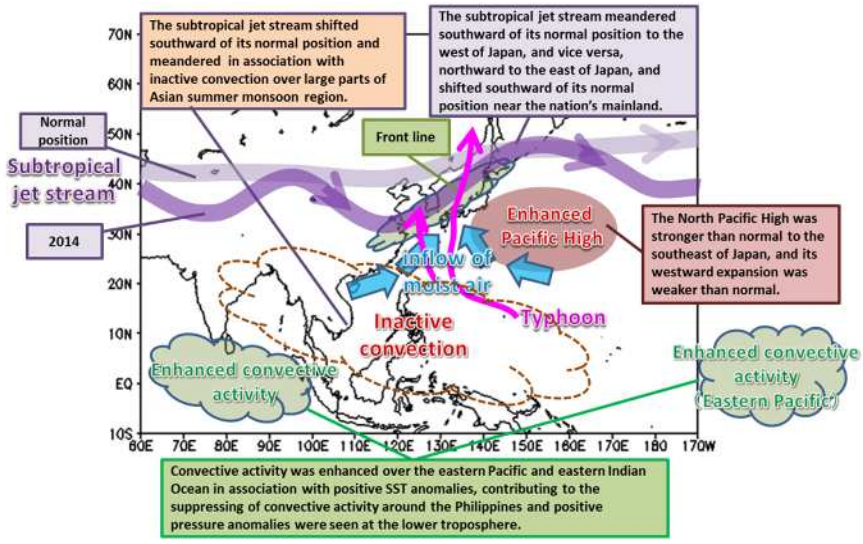

Figure 21 Primary factors contributing to the unseasonable weather conditions of August 2014 in Japan

3. Long-term trends of extreme precipitation events (Figures 22 and 23)

JMA operationally observes precipitation at around 1,300 unmanned regional meteorological observation stations all over Japan (collectively known as the Automated Meteorological Data Acquisition System, or AMeDAS). The annual[3] and monthly (August) numbers of events[4] with precipitation exceeding 50 mm/hour and 80 mm/hour observed at AMeDAS stations are likely to have increased (Figure 22). Data on water vapor presence in Japan based on upper-air observation also show an increasing trend (Figure 23). According to the Intergovernmental Panel on Climate Change (IPCC) Fifth Assessment Report (AR5), extreme precipitation events over most mid-latitude land masses will very likely become more intense and more frequent, and the amount of water vapor in the air will likely increase by 5 to 25% by the end of this century as global mean surface temperatures rise.

From the above, it can be inferred that the increasing trend seen in the number of extreme precipitation events may be linked to global warming. As the period covered by observation records is still relatively short, the addition of future data series is expected to allow further clarification regarding the increasing trend's relationship with global warming.

Climatological regions of Japan

The country has four divisions (northern, eastern, western Japan and Okinawa/Amami) and eleven subdivisions (Hokkaido, Tohoku, Kanto-koshin, Hokuriku, Tokai, Kinki, Chugoku, Shikoku, northern Kyushu, southern Kyushu and Okinawa).

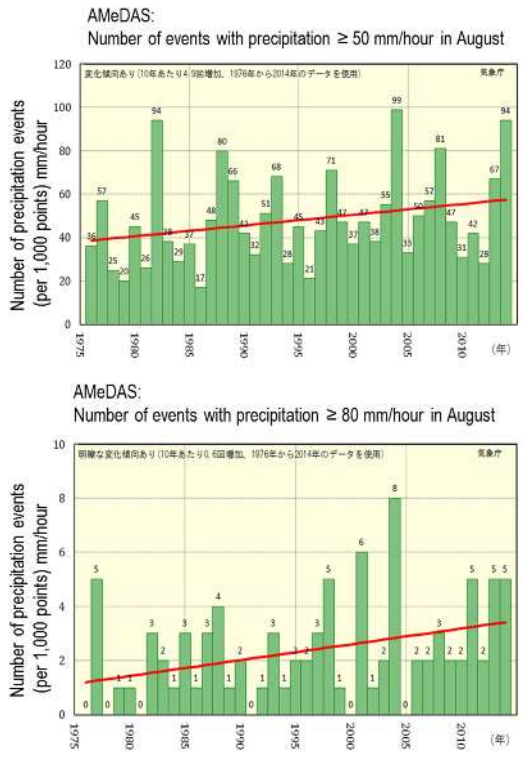

Figure 22 Number of events with precipitation greater than or equal to 50 mm/hour (above) and 80 mm/hour (below) in August from 1976 to 2014 (per 1,000 Automated Meteorological Data Acquisition System (AMeDAS) points)

The green bars indicate values for each year, and the straight red lines indicate the long-term linear trend (statistically significant at a confidence level of 90%).

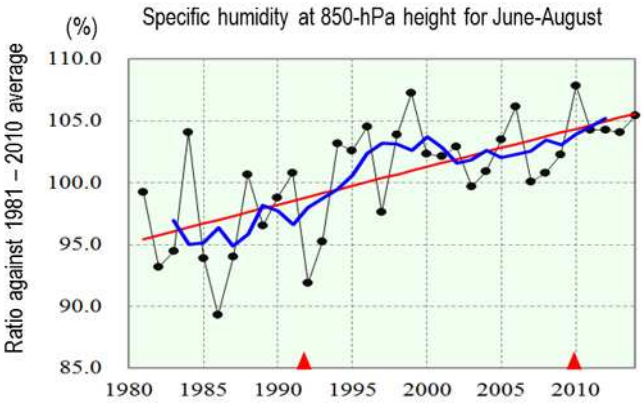

Figure 23 Time-series representations of specific humidity ratios for summer (June – August) at 850 hPa from 1981 to 2014 in Japan

The data are presented as ratios against the baseline (the 1981 – 2010 average).

Note: The term *specific humidity* refers to the mass of water vapor in a unit mass of moist air (g/kg). The data used in this analysis were based on observations made using radiosondes (balloon-borne instrument platforms with a radio-transmitting device) at 13 upper-air observation stations in Japan. The dots show the averages of the data for the 13 stations. The thick blue line indicates the five-year running mean, and the straight red line indicates the long-term linear trend (statistically significant at a confidence level of 95%). The red triangles indicate changes of observation instruments.

[3] See Figure 2.2-7 of the Climate Change Monitoring Report 2013 http://www.data.jma.go.jp/cpdinfo/monitor/2013/pdf/ccmr2013_all.pdf.

[4] There were around 800 AMeDAS stations in 1976, gradually increasing to around 1,300 by 2012. To account for these numerical differences, the number of precipitation events is converted to a per-1,000-station basis.

Launch of New Website on Climate Risk Management

Introduction

Daily life and economic activity are greatly affected by anomalous climatic conditions. The potential for adverse effects from such conditions is referred to as climate risk, and climate risk management (CRM) involves understanding and taking effective measures against it. The Global Framework for Climate Services (GFCS) is intended to enable better management of climate-related risk. To promote better use of climate information in CRM in Japan, JMA has launched a dedicated website at http://www.data.jma.go.jp/gmd/risk/en/index.html, which is also linked to the TCC website. A leaflet on CRM has additionally been published to promote the use of climate information.

New website for CRM support

The new website includes information on the following to support CRM activities in Japan:

- Clarification of the basic CRM concept and related processes
- Good practices in CRM conducted by JMA together with partner organizations in the agriculture and apparel/fashion industries

More details can be found in TCC News No.33 (summer 2013 edition).

Good practices in the apparel/fashion industry

Together with the Japan Apparel Fashion Industry Council (JAFIC), JMA investigated the relationship between fashion items and temperature as well as other weather factors. It was found, for example, that sandal sales tend to increase remarkably when the temperature rises above 15°C (Figure 24). The study included investigation of how two-week forecasts can be used to promote sales and increase profits. In the case of sandals, when the two-week forecast (Figure 25) indicates a high possibility of temperatures exceeding 15°C, footwear sales managers should ensure that there is sufficient stock and arrange frequent replenishment. Floor managers may also wish to prioritize the display of sandals in the selling area. (Some more details can be found on JMA's website.)

JMA began joint research with the Japan Association of Chain Drug Stores to promote the use of climate information in the retail field this year. The results will be posted on the CRM website next year. The Agency will continue its efforts in relation to good practices for CRM in various fields in the future.

(Akira Ito, Climate Prediction Division)

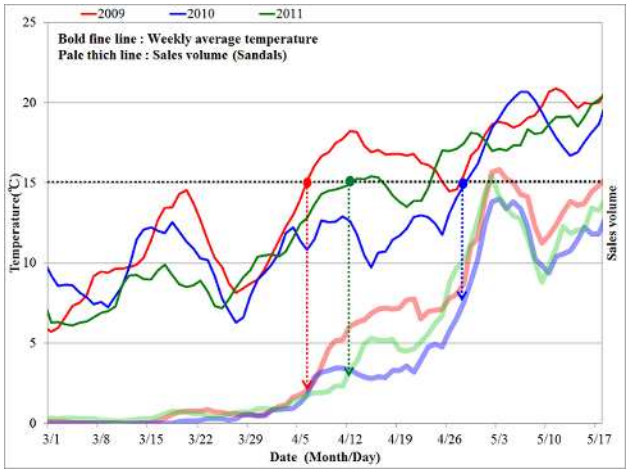

Figure 24 Time-series representation of sandal sales and mean temperature

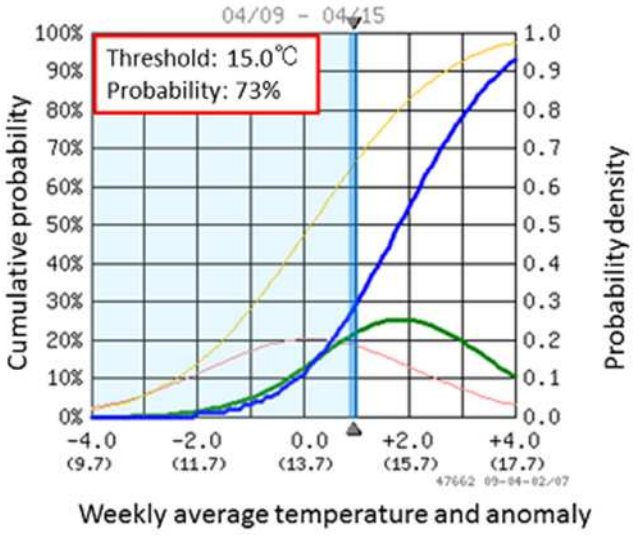

Figure 25 JMA two-week forecast product
Initial date/location: 2nd April 2009, Tokyo
Cumulative probability: Forecast (Blue), Normal (Yellow)
Probability density: Forecast (Green), Normal (Pink)

The Second Session of the East Asia winter Climate Outlook Forum (EASCOF-2)

The World Meteorological Organization (WMO) has initiated the Regional Climate Outlook Forum (RCOF), which brings together experts from a climatologically homogeneous region and provides consensus-based climate predictions and information for the season having socio-economic significance. At the 15th session of the WMO Regional Association II (Asia) in Dec. 2012, the China Meteorological Administration (CMA), the Japan Meteorological Agency, the Korea Meteorological Administration (KMA) and Mongolia's National Agency for Meteorology and Environment Monitoring (NAMEM) jointly announced the establishment of a new WMO sub-RCOF called the East Asia Winter Climate Outlook Forum (EASCOF) as a successor to the Joint Meeting for Seasonal Prediction of the East Asian Winter Monsoon, which was held in autumn every year from 2000 to 2012.

From 29 to 31 October 2014, the second session of EASCOF (EASCOF-2) took place at JMA's Headquarters in Tokyo.

More than 30 experts from China, Japan, Mongolia and the Republic of Korea attended the session, sharing their recent understandings on phenomena related to seasonal prediction of the East Asian winter monsoon as well as discussing and summarizing seasonal outlooks for the coming winter. The session's discussions are expected to be useful for participating NMHSs in the formulation of their own seasonal outlooks. Recent research findings presented at the event helped to enhance understanding of phenomena related to the East Asian winter monsoon and related predictability. These phenomena include the global warming hiatus, interaction between the troposphere and the stratosphere, ENSO and the influence of Arctic sea ice.

The third session will be hosted by KMA in autumn 2015.

(Atsushi Goto, Tokyo Climate Center)

Any comments or inquiry on this newsletter and/or the TCC website would be much appreciated. Please e-mail to tcc@met.kishou.go.jp.

(Editors: Teruko Manabe, Atsushi Goto and Yasushi Mochizuki)

Tokyo Climate Center (TCC), Japan Meteorological Agency
Address: 1-3-4 Otemachi, Chiyoda-ku, Tokyo 100-8122, Japan
TCC Website: http://ds.data.jma.go.jp/tcc/tcc/index.html